

Sensitivity of Low-Energy π^\pm Inelastic Scattering

R. Tacik, K. L. Erdman, R. R. Johnson, and H. W. Roser

Physics Department, University of British Columbia, Vancouver, British Columbia V6T2A6, Canada

and

D. R. Gill and E. W. Blackmore

TRIUMF, Vancouver, British Columbia V6T2A3, Canada

and

R. J. Sobie and T. E. Drake

Physics Department, University of Toronto, Toronto, Ontario M5S 1A7, Canada

and

S. Martin

Kernforschungsanlage, Institut für Kernphysik, D-5170 Jülich, West Germany

and

C. A. Wiedner

Max-Planck Institut für Kernphysik, D-6900 Heidelberg, West Germany

(Received 16 December 1983)

A distorted-wave impulse-approximation calculation for 50-MeV π^\pm inelastic scattering to the 2_1^+ state in ^{26}Mg has been performed. The calculation shows greater sensitivity to the separate neutron and proton deformations than is seen with any other nuclear probe. A fit to the measured differential cross sections gives the value of 0.83 ± 0.06 for the ratio of neutron to proton matrix elements for this state. This is in agreement with the values deduced with other probes.

PACS numbers: 25.80.Fm, 27.30.+t

Because of its availability in different charge states, and its interaction properties, there has been much hope put on the pion as a probe of nuclear structure.¹ The bulk of the pion scattering data has been taken at ≈ 160 MeV incident pion energy. The total pion-nucleon (πN) cross section peaks near this energy, because of the presence of the $\Delta(1232)$ resonance. The fact that it is much smaller at lower incident pion energies has formed the basis for the much used argument² that a low-energy pion has a much longer mean free path in nuclear matter, and thus should be a much better probe of nuclear structure. This point of view is in accord with the results of Friedman.³

There is, however, a much more compelling argument in favor of the low-energy pion as a nuclear probe. Figure 1 illustrates the ratio of $d\sigma(\pi^+p)/d\Omega$ to $d\sigma(\pi^-p)/d\Omega$ as a function of c.m. scattering angle, for various incident pion energies, calculated with the phase shifts of Arndt and Roper.⁴ Whereas this ratio is quite flat at $T_\pi = 160$ MeV, it rises dramatically at $T_\pi = 50$ MeV, reaching a maximum of 400:1. The average value is 20. The con-

stant factor of ≈ 9 between the (π^+p) and (π^-p) differential cross sections at $T_\pi = 160$ MeV stems from an overall factor of 3 in the ratio of the scattering amplitudes. At resonance energies, scattering is dominated by the P_{33} πN partial wave, and the factor of 3 is a Clebsch-Gordan coefficient, present because (π^+p) exists in a pure isospin- $\frac{3}{2}$ state, while (π^-p) exists in a mixture of isospin- $\frac{3}{2}$ and isospin- $\frac{1}{2}$ states. At lower incident pion energies, this overall factor is still present, but there are three πN phase shifts (i.e., $S_{11} = 6.72^\circ$, $S_{31} = -5.36^\circ$, and $P_{33} = 6.26^\circ$)⁴ that contribute to the total amplitude, which are similar in magnitude, but differ in sign and thus can interfere, and produce the observed effect.

When one considers pion-nucleus scattering, the situation is complicated by true pion absorption, which cannot occur on a single nucleon. Nevertheless, at resonance energies, the general features of pion-nucleus scattering are well described by the Kisslinger⁵ optical potential. This potential is based on a first-order expansion of the multiple scattering series, and its coefficients are obtained from πN

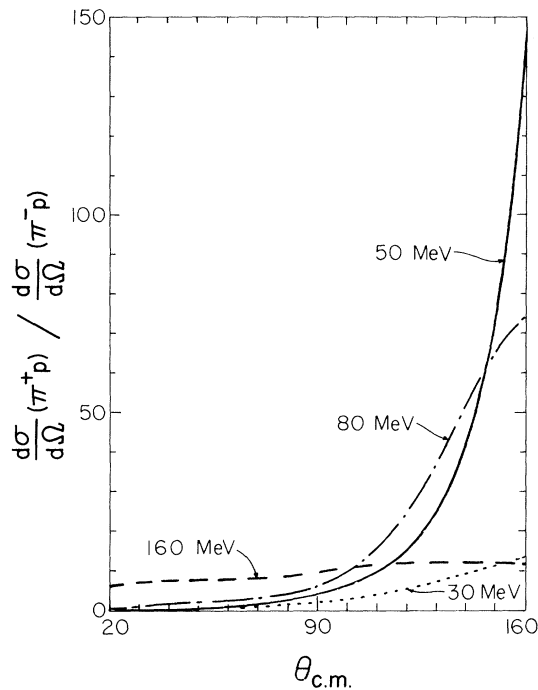


FIG. 1. Ratio of (π^+p) to (π^-p) differential cross sections from Ref. 4. Solid curve is for $T_\pi=50$ MeV, dashed curve for $T_\pi=160$ MeV, dash-dotted curve for $T_\pi=80$ MeV, and dotted curve for $T_\pi=30$ MeV.

phase shifts. Thus, it may not be surprising to find the same sensitivity in resonance-energy pion-nucleus scattering as in the pion-nucleon case.

At lower pion energies, the simple Kisslinger model cannot be made to fit the existing elastic-scattering data without altering its coefficients outside the values obtained from πN phase shifts. The solution is to add extra terms to the potential, to account for various effects, including absorption and higher-order terms in the multiple scattering series. The question then arises as to whether or not the same sensitivity seen in πN scattering is still present. In this Letter we present evidence that it is.

This conclusion is based on the results of a distorted-wave impulse-approximation calculation for the inelastic scattering of 50-MeV π^\pm to the first 2^+ state in ^{26}Mg , as well as the experimentally determined angular distributions. The calculation employed the full optical potential of Stricker, McManus, and Carr,⁶ and separate deformation parameters for the neutron and proton nuclear transition densities. The results fit the data well, and show remarkable sensitivity to these deformation

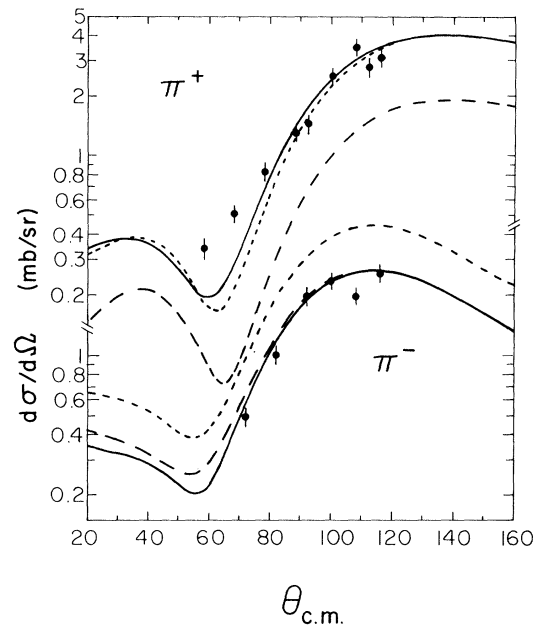


FIG. 2. Experimental and calculated angular distributions for π^\pm scattering to the 2_1^+ state of ^{26}Mg . The solid curves use the best-fit values of $\beta_p=0.655$ and $\beta_n=0.465$. The long-dashed curves have β_p lowered to 0.459. The short-dashed curves have β_n increased to 0.605.

parameters.

The experiment was performed on the M13 channel⁷ at TRIUMF. The scattered pions were detected with the quadrupole-quadrupole-dipole spectrometer.⁸ A self-supporting metallic ^{26}Mg target enriched to 99.4% with a thickness of 300 mg/cm² was used. The energy resolution of the spectrometer was ≈ 1.1 MeV (full width at half maximum) which necessitated some peak fitting. Full experimental details will be presented in another paper. The error bars associated with the data shown in Fig. 2 include statistical errors, systematic errors due to uncertainties in peak fitting, and overall normalization errors.

The calculation was performed with a modified version of the code DWPI.⁹ The first modification involved using the full optical potential of Ref. 6 to generate the distorted waves. All results presented in this Letter used the Ref. 6 "set E" optical potential coefficients, along with Fermi nuclear matter distributions with the parameters determined by Gyles.¹⁰ The second modification was involved in the expansion of the potential into spherical and deformed parts. The inelastic scattering is calculated

from the matrix elements of the deformed part, which we have written as (in the notation of Ref. 6)

$$\begin{aligned} \left(\frac{2E}{\hbar^2 c^2} \right) \frac{1}{4\pi} V^{(1)} = & p_1 \left(-b_0 F_A + \epsilon b_1 F_D \right) - 2p_2 B_0 \rho_A F_A \\ & + \nabla^2 \left\{ \frac{p_1 - 1}{2p_1} [-c_0 F_A + \epsilon c_1 F_D] - C_0 \frac{p_2 - 1}{p_2} \rho_A F_A \right\} \\ & + \nabla \left\{ \frac{c_0 F_A / p_1 - \epsilon c_1 F_D / p_1 + 2C_0 \rho_A F_A / p_2}{[1 + 4\pi\lambda/3(c_0 \rho_A / p_1 - \epsilon c_1 \rho_D / p_1 + C_0 \rho_A^2 / p_2)]^2} \right\} \nabla, \end{aligned}$$

where $\rho_{A,D} = \rho_n \pm \rho_p$, $F_{p,n} = a_{0p,n} (\partial \rho_{p,n} / \partial a) |_{a_{0p,n}}$, and

$$F_{A,D} = (\beta_n F_n \pm \beta_p F_p) Y_0^L.$$

The deformation parameters β_p and β_n were varied in order to minimize the χ^2 of the fit to the π^\pm data simultaneously. The solid curves in Fig. 2 represent the calculation with the best-fit values of $\beta_p = 0.655$ and $\beta_n = 0.465$. The long-dashed curves are the result of the calculation with β_p reduced by 30%, while the short-dashed curves have β_n increased by 30%. The extreme sensitivity of the π^+ (π^-) calculation to variations in β_p (β_n), its insensitivity to variations in β_n (β_p), as well as the opposite direction of the two effects are evident.

In an effort to quantify this sensitivity, we may adopt the parametrization of Iversen,¹¹ and write the ratio of total π^\pm cross sections as

$$\frac{\sigma^+}{\sigma^-} = \left(\frac{b_p^+ Z \beta_p + b_n^+ N \beta_n}{b_p^- Z \beta_p + b_n^- N \beta_n} \right)^2,$$

where $b_{p,n}^\pm$ are the interaction strengths of π^\pm , and are measures of their sensitivity to the protons and neutrons in the nucleus. Figure 3 illustrates the results of our DWPI calculation along with curves computed with the above formula for various values of $b_p^+ / b_n^+ = b_n^- / b_p^-$. The results of the calculation are shown as a shaded region because they have some dependence on the individual values of β_p and β_n , and not just their ratio. It is evident from Fig. 3 that $b_n^- / b_p^- \approx -20$. Bernstein, Brown, and Madsen¹² discuss the interaction strengths for other probes. These are 1.0 for α particles; 0.83 and 0.95 for 800-MeV and 1-GeV protons; and 3 ($\frac{1}{3}$) for low-energy protons (neutrons), and resonance-energy π^- (π^+). Thus, both the magnitude and the sign of our result indicate that low-energy pions are more sensitive to relative neutron and proton matter distributions than any of the above-mentioned probes.

This sensitivity enables us to determine the ratio β_n / β_p with a relatively small uncertainty. Figure 4

is a contour plot of the χ^2 values for the simultaneous fit of the measured π^\pm inelastic differential cross sections. Our result is $\beta_n / \beta_p = 0.71 \pm 0.05$. Given that the ratio of neutron to proton matrix elements for the transition is related to the ratio of deformation parameters by $M_n / M_p = N \beta_n / Z \beta_p$, our result is $M_n / M_p = 0.83 \pm 0.06$. The values obtained with other probes are 0.72 ± 0.15 (electromagnetic decay, mirror nuclei)¹³; 0.80 ± 0.17 [(α, α')]¹⁴; 0.62 ± 0.14 (resonance-energy π^\pm)¹⁵; and 0.74 ± 0.12 [800-MeV (p, p')]¹⁶. The present result is slightly higher than, though not inconsistent with, all of these.

As seen with other probes,¹⁷ the separate values

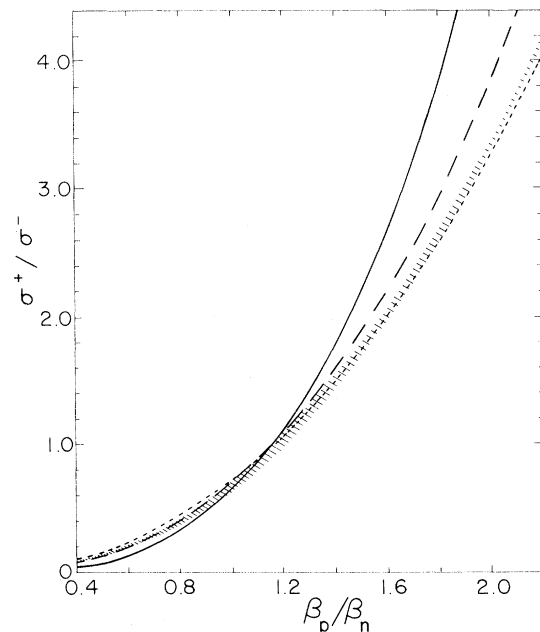


FIG. 3. Ratio of π^\pm total cross sections. Shaded region is the result of our distorted-wave impulse-approximation calculation. Curves are from the formula given in the text. Solid line uses $b_p^+ / b_n^+ = -5.0$; long-dashed line uses $b_p^+ / b_n^+ = -10.0$; short-dashed line uses $b_p^+ / b_n^+ = -25.0$.

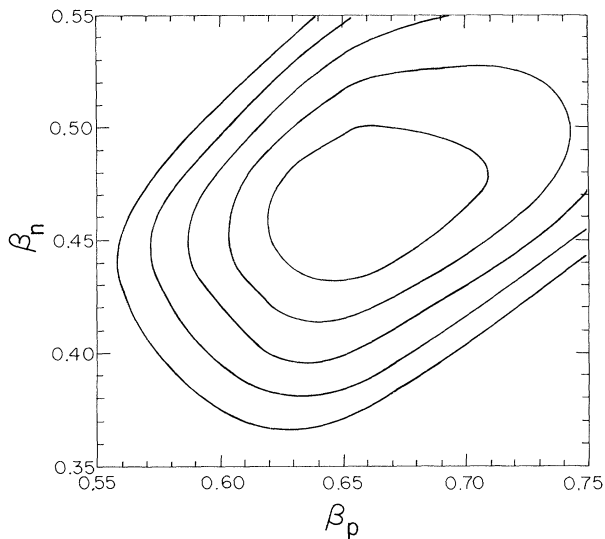


FIG. 4. Contour plot of the reduced χ^2 values for the simultaneous fit of the measured π^+ differential cross sections. The minimum is at $\chi^2=3.7$, and each contour line represents an increase of 1.0.

of β_p and β_n extracted from fits to the data are not necessarily uniquely determined, but depend on the optical potential parameters used in the fitting calculation. The present parameter set has a basis both in theory and in its ability to fit a large set of elastic-scattering data,⁶ which, in our view, justifies its use. In any case, although an exhaustive study has not been completed, preliminary investigations indicate that the extracted ratio β_n/β_p is not affected by minor variations in the optical potential parameters. An exhaustive study should also include possible coupled-channel effects.

Data on 50-MeV π^+ inelastic scattering to other states and nuclei are presently being analyzed, and more measurements are in progress. The availabili-

ty of more data will certainly lead to a better understanding of the interaction. The present results indicate that we will be able to exploit the high sensitivity of the pion probe to extract useful nuclear structure information.

This work was supported in part by the Natural Sciences and Engineering Research Council of Canada.

-
- ¹R. H. Landau, Nucl. Phys. **A335**, 289 (1980).
²S. A. Dytman *et al.*, Phys. Rev. C **19**, 971 (1979); B. M. Freedman *et al.*, Phys. Rev. C **23**, 1134 (1981).
³E. Friedman, Phys. Rev. C **28**, 1264 (1983).
⁴R. A. Arndt and L. D. Roper, SAID Scattering Analysis Interactive Dial-in program, Centre for Analysis of Particle Scattering, Virginia Polytechnic Institute and State University Internal Report No. CAPS-80-3, 1982 (unpublished).
⁵L. S. Kisslinger, Phys. Rev. **98**, 761 (1955).
⁶K. Stricker, H. McManus, and J. A. Carr, Phys. Rev. C **19**, 929 (1979), and **22**, 2043 (1980), and **25**, 952 (1982).
⁷C. J. Oram *et al.*, Nucl. Instrum. Methods **179**, 95 (1981).
⁸R. J. Sobie *et al.*, TRIUMF Report No. TRI-PP-83-63, 1983 (to be published).
⁹R. A. Einstein and G. A. Miller, Comput. Phys. Commun. **11**, 95 (1976).
¹⁰W. Gyles, Ph.D. thesis, University of British Columbia, 1983 (unpublished).
¹¹S. Iversen *et al.*, Phys. Rev. Lett. **40**, 17 (1978).
¹²A. M. Bernstein, V. R. Brown, and V. A. Madsen, Phys. Lett. **103B**, 255 (1981), and **106B**, 259 (1981).
¹³A. M. Bernstein, V. R. Brown, and V. A. Madsen, Phys. Rev. Lett. **42**, 425 (1979).
¹⁴A. M. Bernstein, in *Advances in Nuclear Physics*, edited by M. Baranger and E. Vogt (Plenum, New York, 1969), Vol. 3, p. 325.
¹⁵C. A. Wiedner *et al.*, Phys. Lett. **97B**, 37 (1980).
¹⁶G. S. Blanpied *et al.*, Phys. Rev. C **25**, 422 (1982).
¹⁷A. Saha *et al.*, Phys. Lett. **114B**, 419 (1982).